Journal of Geochemical Exploration 175 (2017) 110–119

Contents lists available at ScienceDirect

Journal of Geochemical Exploration

journal homepage: www.elsevier.com/locate/gexplo

The impact of natural and anthropogenic factors on groundwater quality in an active volcanic/geothermal system under semi-arid climatic conditions: The case study of Methana peninsula (Greece)

W. D'Alessandro [a,*], S. Bellomo [a], L. Brusca [a], K. Kyriakopoulos [b], S. Calabrese [c], K. Daskalopoulou [c]

[a] Istituto Nazionale di Geofisica e Vulcanologia – sezione di Palermo, Italy
[b] National and Kapodistrian University of Athens, Dept. of Geology and Geoenvironment, Greece
[c] University of Palermo, Dipartimento di Scienze della Terra e del Mare (DiSTeM), Italy

ARTICLE INFO

Article history:
Received 2 May 2016
Revised 12 December 2016
Accepted 5 January 2017
Available online 7 January 2017

Keywords:
Hydrogeochemistry
Volcanic aquifers
Salinization
Stable isotopes
Trace elements

ABSTRACT

A comprehensive hydrogeochemical study of the cold and thermal groundwaters of the presently quiescent volcanic system at Methana was undertaken that involved collecting 71 natural water samples. Methana is a peninsula in Peloponnesus, Greece whose arid climate and hydrological situation is similar to that of the nearby small islands of the Aegean Sea. Similarly, the chemical and isotopic compositions of its water are dominated by the mixing of seawater with meteoric water both through direct intrusion and meteoric recharge. However, the simple mixing trends at Methana are modified by water–rock interaction processes, enhanced by the dissolution of endogenous CO_2, which lead to strong enrichments in alkalinity, Ca, Ba, Fe and Mn. The thermal waters show very high salinity that is sometimes close to that of seawater [total dissolved solids (TDS) = 8.5–40 g/l]. Although the cold groundwaters sometimes also show elevated TDS values (up to 6.3 g/l), their overall quality is acceptable due to the trace metal and nitrate contents mostly being below acceptable limits. While the saltiest groundwaters are not acceptable for human consumption, they are used for irrigation without exerting toxic effects on plants, which is probably due to the high permeability of the soils not supporting salt accumulation and salinity-resistant crops being cultivated.

© 2017 Elsevier B.V. All rights reserved.

1. Introduction

Groundwater is a precious resource that sustains the life of the ever-growing population of the earth. Its composition undergoes various transformations induced by natural and anthropogenic hydrological, geochemical and biological processes along its evolutionary path (Salama et al., 1999; Custodio, 2010). Salinization due to seawater intrusion and/or sea-spray deposition can severely degrade the groundwater quality in coastal areas and on islands, especially in arid areas (Custodio, 2010; Kuiper et al., 2015; Zhang et al., 2015). This is a particularly widespread problem in the highly populated arid and semi-arid zones of the Mediterranean region (Milnes and Renard, 2004; D'Alessandro et al., 2011 and references therein). Greece is characterized by huge extensions of the surface coastal areas and hundreds of inhabited islands, which makes it particularly vulnerable to salinization problems (Dazy et al., 1997; Petalas and Lambrakis, 2006).

Groundwater quality issues can be exacerbated if the area hosts an active volcanic or geothermal system (Aiuppa et al., 2003; Koh et al., 2007; Cordeiro et al., 2012; Freire et al., 2014; Jung et al., 2014). The geological youth and high geodynamical activity of the Hellenic territory, (Pe-Piper and Piper, 2002) make it particularly vulnerable to this problem. The country is characterized by many recent and active volcanic systems as well as widespread geothermal areas that release fluids that often cause water quality problems in the shallow aquifers (Dazy et al., 1997; Petalas et al., 2006; Duriez et al., 2008; Kontis and Gaganis, 2012).

Methana is a peninsula with an area of about 44 km^2 on the north-eastern coast of Peloponnesus in Greece. It is close to being an island since it is joined to the mainland by an isthmus that is only 300 m wide. It has no perennial springs or streams, and belongs to the driest south-eastern region of Greece with an annual rainfall of <400 mm (Pantelouris, 1980). This makes water shortages very common, and in the geographic literature Methana has been described as "a rough and rocky place" (quoted in Mee and Forbes, 1997). Its hydrology is actually closer to that of the arid islands of the nearby Cyclades Archipelago (Dazy et al., 1997) than to the Peloponnesus to which it geographically belongs. Despite these harsh environmental conditions, the peninsula has a settlement history starting from prehistoric times. Stable human presence has been archeologically documented since the Early Helladic period at the end of the fourth millennium BC (Mee and Forbes, 1997). The high fertility of its young volcanic soils is probably one of the main

* Corresponding author.
E-mail address: walter.dalessandro@ingv.it (W. D'Alessandro).

http://dx.doi.org/10.1016/j.gexplo.2017.01.003
0375-6742/© 2017 Elsevier B.V. All rights reserved.

reasons that attracted its earliest inhabitants. In contrast with the neighbouring parts of the Peloponnesus, the rocks outcropping at Methana are mostly of volcanic origin.

The entire peninsula is hilly, with a highest altitude of 740 m at Mt. Chelona. Flat land is rare, being restricted to a few upland basins and small coastal plains. These constraints have led to more than the half of the entire surface of the peninsula being covered with terraces to permit cultivation of the slopes. These terraces were built generally up to altitudes of about 400 m, but in the central area they extend to above 600 m (James et al., 1997). These constructions have permanently modified the geomorphology of the peninsula to allow widespread agricultural exploitation as well as protecting its slopes from rapid erosive processes. For centuries agricultural production was restricted to products that needed no irrigation, mainly wine and olives. The situation changed markedly during the first half of the 20th century when many irrigated crops were introduced. This dramatic change was due to a series of concurring factors: the favourable climate for the production of early crops, the closeness to the important and fast-growing consumer market of Athens, and the motorization of ships allowing regular and secure transportation to markets (Forbes, 1997). To obtain the necessary irrigation water, many wells were sunk down to the water table in areas close to the coast. The water in these wells, which were up to 20 m deep, was brought to the surface by an endless chain of buckets powered by donkeys or mules. The installation in the 1960s of a pipeline bringing water through the isthmus from the nearby plain of Troezen solved the problem of an inadequate water supply, but many of the wells excavated in that period are still used for irrigation and operated with electrically powered pumps.

The youthfulness of the volcanic system at Methana—apart from the historic eruptive activity that emplaced the dome and lava flows of Kammeno Vouno in 230 BCE—is corroborated by the presence of hydrothermal manifestations (Pe-Piper and Piper, 2002; D'Alessandro et al., 2008). The exploitation of thermal springs, which begun in Roman times (Mee and Forbes, 1997), represents nowadays another important source of income for its inhabitants.

A few studies have performed chemical analyses of the thermal waters (Pertessis, 1925; von Leyden, 1940; Minissale et al., 1997; Lambrakis and Kallergis, 2005; Dotsika et al., 2010), but no comprehensive study of the cold and thermal groundwaters at Methana has been reported in the scientific literature. In this paper we present the findings obtained in new chemical and isotope analyses of many groundwater samples collected at the peninsula during the period 2004–2009. Such dataset allowed to discriminate at least two aquifers, one shallow, cold with low to medium salinity (<6.3 g/l), and one deeper, thermal with higher salinity (8.5–40 g/l). Chemical and isotopic analyses are used to delineate the hydrologic circuits and to describe the volcanic gas-water-rock interactions responsible of their geochemical evolution. The suitability of the cold waters for human consumption and use in irrigation is also discussed.

2. Study area

The almost circular outline of Methana is broken in the north-west by the projection formed by the hill of Panagia, a mass of grey limestone (from Upper Triassic to Lower Jurassic), and on the south by Asprovouni limestones (from Upper Jurassic to Cretaceous), of which the isthmus is an elongation (Dietrich and Gaitanakis, 1995) (Fig. 1). These sedimentary sequences together form the basement underneath the volcanic complex at depths of down to 1000 m below sea level (Volti, 1999).

The Methana volcano belongs to the volcanic group of the Saronic Gulf, which represents the north-west part of the south Aegean active volcanic arc and comprises also the volcanic centres of Sousaki, Aegina and Poros (Fytikas et al., 1986). This area is characterized by active extensional tectonics, although it is seismically less active than the adjacent Corinth Gulf area (Makris et al., 2004).

The volcanic activity at Methana probably started at the Pliocene–Pleistocene boundary, although the oldest dated rocks have ages of about 0.9 Ma. Very few radiometric ages for the volcanic rocks at Methana have been reported in the literature (Pe-Piper and Piper, 2002). Instead, the volcanic history of the peninsula has mainly been reconstructed from geomorphological data. Dietrich and Gaitanakis (1995) attributed an old undated volcanic series to the late Pliocene followed by seven groups of volcanic rocks of the Quaternary period. Radiometric measurements of samples from the most recent of these groups gave ages of 0.29–0.38 Ma, while the older series gave ages of 0.55–0.9 Ma (Pe-Piper and Piper, 2002). The most recent volcanic activity was a flank eruption described by Strabo (Stothers and Rampino, 1983) that produced andesitic lavas at Kammeno Vouno around 230 BCE.

The volcanic sequences of the peninsula consist principally of andesite and dacite lava domes and flows that extend radially from its centre (Pe-Piper and Piper, 2002). The volcanic rocks are mainly calc-alkaline andesites and dacites, with rare basaltic andesites, and generally have a K content that is lower than those of the older adjacent volcanic systems of Aegina and Poros. Plagioclase, clinopyroxene, orthopyroxene and magnetite constitute the phenocryst paragenesis of andesites,

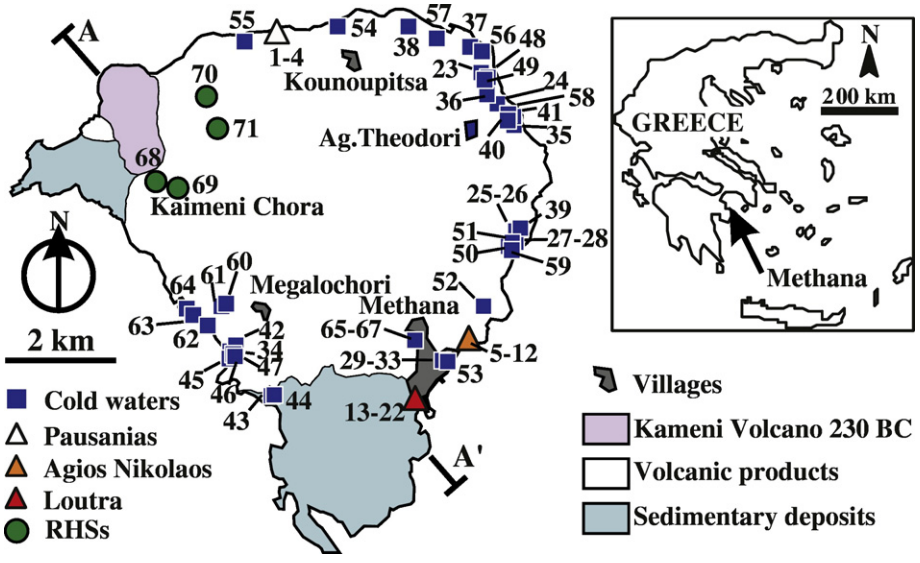

Fig. 1. Simplified geological map of Methana and location of the sampling sites. A–A′ represents the trace of the profile shown in Fig. 8.

whereas in the dacites, plagioclase and magnetite are associated with hornblende and biotite (Francalanci et al., 2005).

Three groups of thermal manifestations can be recognized at Methana: Loutra, Agios Nikolaos and Pausanias (Fig. 1). The first two are on the south-eastern coast along an active tectonic structure that is also characterized by gas bubbling in seawater, anomalous soil gas fluxes and hydrothermally altered rocks (D'Alessandro et al., 2008). The southernmost manifestation, Loutra, comprises a group of H_2S-rich springs issuing from fractures of the Asprovouni limestones close to the coast or directly under the sea, and their waters are exploited by a commercial spa. Agios Nikolaos spring is about 2 km further north, and it is also close to the sea and exploited by a commercial spa. The last thermal spring, Pausanias, issues very close to the sea along another active tectonic structure on the northern coast of the peninsula. The ancient writer Pausanias, to whom the spring is dedicated, stated that these thermal waters appeared soon after the volcanic eruption around 230 BCE. All three thermal groups are characterized by intense CO_2 degassing producing a strong gas hazard that led to two fatalities in August 2009 (D'Alessandro and Kyriakopoulos, 2013).

3. Sampling and analytical methods

Seventy-one water samples were collected at Methana peninsula (Fig. 1), 22 of them were taken from the thermal springs (samples 1 to 22 in Table S1), 45 from the cold aquifer (samples 23 to 67) and 4 from rainwater harvesting systems (RHSs; samples 68 to 71). The RHS samples were collected in order to obtain insight into the chemical and isotopic compositions of the meteoric recharge. The cold-groundwater samples were taken from many of the wells dug at the peninsula. The samples were collected using a pump where this was possible; in other cases a well-sampling bailer was lowered to the water table.

The water temperature, pH, electric conductivity (EC) and redox potential (Eh) were measured in the field using portable instruments. Chemical and isotope analyses were carried out at the laboratories of INGV-Palermo. Total alkalinity was determined by titrating unfiltered samples with 0.1 M HCl and methyl orange indicator. Major anions (Cl^-, NO_3^- and SO_4^{2-}) were determined by Ionic Chromatography of filtered samples. Major cations (Na^+, K^+, Mg^{2+} and Ca^{2+}) determined by Ionic Chromatography, Si determined by Inductively Coupled Plasma (ICP) Optical Emission Spectrometry (OES), and minor and trace elements (Li, B, Al, V, Cr, Mn, Fe, Co, Ni, Cu, Zn, As, Se, Rb, Sr, Mo, Cd, Sb, Cs, Ba, Pb and U) determined by ICP Mass Spectrometry (MS) were quantified in samples filtered using 0.45-μm cellulose acetate filters and acidified using 0.2% HNO_3. Spectrophotometric methods were used to determine NH_4 via Berthelot's reaction. The oxygen and hydrogen isotopic compositions were analysed on unfiltered water samples using Analytical Precision AP 2003 and FinniganMAT Delta Plus IRMS devices, respectively. The isotopic ratios are expressed as the deviation per mil (δ‰) from the reference V-SMOW. The uncertainties 1σ were ±0.1% for $\delta^{18}O$ and ±1% for δD.

4. Results and discussion

The results obtained in the chemical and isotope analyses are summarized in Table 1 as minimum, median and maximum values for the three thermal-water sampling sites, the cold groundwaters and the RHSs; the complete analytical results are given as supplementary material in Table S1 together with the saturation indexes of some mineral phases and CO_2 partial pressure calculated with PHREEQC (Parkhurst and Appelo, 2010). Thermal waters display temperatures from 19.0 to 37.5 °C, pH values from 5.80 to 6.72, and EC values from 10,200 to 58,000 μS/cm. Two of the thermal sites (Pausanias and Loutra) have strongly negative Eh values, from −300 to −210 mV, while the third one (Agios Nikolaos) has positive values (110–179 mV). Cold-groundwater samples display lower temperatures (16.5–26.0 °C) and EC values (734–7800 μS/cm) and have a wider range of pH values (5.89 to 8.32) and positive Eh values (3–214 mV), with the exception of a single negative value of −142 mV.

4.1. Stable isotopes

The isotopic composition of the analysed waters ranges from −7.4 to 1.3‰ for $\delta^{18}O$ and from −42 to 5‰ for δD. At present we have no isotope data on the meteoric recharge at the peninsula. Indeed, even precipitation amount data are lacking: the only data (600 and 390 mm during the agricultural seasons of 1972–1973 and 1973–1974, respectively) have been reported by James et al. (1997). Some insight into the isotopic composition of the meteoric recharge at Methana can be obtained by using both the data of the samples collected in the RHSs and the literature data of the nearby Athens region (Argiriou and Lykoudis, 2006; IAEA, 2015) and Argolis Peninsula (Matiatos and Alexopoulos, 2011). The plot of δD vs. $\delta^{18}O$ in Fig. 2a indicates that points representative of the RHSs fall between the Global Meteoric Water Line ($\delta D = 8 \times \delta^{18}O + 10$) and the Eastern Mediterranean Meteoric Water Line ($\delta D = 8 \times \delta^{18}O + 22$; Gat and Carmi, 1970), and thereby define a Local Meteoric Water Line (LMWL; $\delta D = 8 \times \delta^{18}O + 18$) that is typical for the central Mediterranean region (D'Alessandro et al., 2004). Rainwaters of the Athens region (Argiriou and Lykoudis, 2006; IAEA, 2015) and Argolis Peninsula (Matiatos and Alexopoulos, 2011) define LMWLs ($\delta D = 7.4 \times \delta^{18}O + 10.4$ and $\delta D = 7.6 \times \delta^{18}O + 13.6$, respectively) that do not differ significantly from that obtained from the RHSs data. Most of the data for the cold groundwaters appear close to the above-defined LMWLs, representing evidence of a prevailing origin through meteoric recharge. In contrast, the thermal waters and some of the cold groundwaters define a mixing line whose end members are the seawater of the Saronikos Gulf (Dotsika et al., 2010; Matiatos and Alexopoulos, 2011) and the local meteoric recharge (Fig. 2a). Seawater intrusion is quite common in coastal aquifers, especially in arid environments where overexploitation can easily exacerbate this process (Dazy et al., 1997). Furthermore, geothermal systems close to the coast nearly always display a prevailing seawater component. In this case seawater intrusion is generally independent from anthropogenic causes, being mainly related to convective movements of the geothermal fluids within the reservoir (Grassi et al., 1995; Celico et al., 1999). Moreover, only naturally escaping thermal waters are currently exploited at Methana.

The present data do not support any contribution of an arc-type magmatic component as previously reported by Dotsika et al. (2010). This magmatic component was poorly constrained and was detected at low percentages, and mostly in samples collected before 1991. It is possible that the upwelling of the magmatic component decreased in recent times or even disappeared due to modifications of the shallow hydrologic circuit as a consequence of construction work that took place in the area in 1991, which also caused a decrease in the output temperature (Dotsika et al., 2010).

The plot of $\delta^{18}O$ vs. Cl in Fig. 2b shows that while thermal waters can still be defined by mixing between the Aegean seawater and the local meteoric recharge, the data for some of the cold groundwaters appear well above this line, despite these waters being relatively rich in Cl. These samples (A in Fig. 2b) were collected from very shallow wells (depths of 1–5 m) that are not exploited and whose large diameters facilitate exchange with atmosphere. Their peculiar composition is probably caused by intense evaporation as highlighted by their $^{18}O/Cl$ ratios typical of evaporating lakes in the Mediterranean area (Aiuppa et al., 2007).

The average recharge altitudes for the Methana cold groundwater can be calculated with the $\delta^{18}O$ lapse rate of −0.45‰ for each 100 m obtained by Matiatos and Alexopoulos (2011) for the nearby Argolis Peninsula. Excluding the samples with $\delta^{18}O$ values higher than −5.0‰, which are affected by significant secondary processes (evaporation, mixing with seawater), the average recharge altitudes range from about 270 to 700 m. The median value of the recharge altitude is around 500 m, which is about 200 m higher than the average elevation of the

Table 1
Chemical and isotopic composition of the water samples collected at Methana.

Sample		T °C	pH	cond µS/cm	Eh mV	Na mg/l	K mg/l	Mg mg/l	Ca mg/l	F mg/l	Cl mg/l	NO_3 mg/l	SO_4 mg/l	Alk mg/l	SiO_2 mg/l	TDS mg/l	$\delta^{18}O$ ‰	$\delta^{2}H$ ‰
Pausanias	Median	27.4	6.21	38,900	−230	10,450	392	1065	910	0.19	18,500	0.50	2190	1445	72.4	35,185	−0.2	−5
	Min	19.0	6.09	32,400	−250	7480	264	840	743	0.07	13,700	0.50	1720	1170	63.3	25,987	−1.0	−7
	Max	30.9	6.42	50,000	−210	11,000	406	1210	1009	0.22	20,500	0.50	2460	1700	83.9	38,040	0.3	−3
Ag. Nikolaos	Median	36.1	6.34	13,050	147	2540	129	309	409	0.13	4375	0.50	711	1205	138	9829	−5.2	−29
	Min	27.5	6.08	10,200	110	2130	110	277	385	0.05	3670	0.50	629	1140	134	8514	−5.7	−32
	max	37.5	6.72	17,700	179	3000	147	341	464	0.20	4820	13.0	780	1340	142	10,966	−5.0	−27
Loutra	Median	30.9	6.05	44,150	−285	10,150	456	1110	872	0.65	18,500	0.50	2450	988	51.6	34,403	−0.1	−4
	Min	29.7	5.80	23,300	−300	4400	215	520	467	0.26	8040	0.50	1100	915	40.7	15,843	−3.5	−20
	Max	33.5	6.43	58,000	−260	11,700	556	1350	1030	0.70	22,000	37.5	2760	1100	81.3	40,323	1.3	5
Cold GW	Median	20.2	6.97	2340	149	338	22.3	76.9	134	0.11	694	14.9	99.4	451	87.8	1794	−6.4	−35
	Min	16.5	5.89	734	−142	49.7	6.26	20.9	40.3	0.05	53.5	0.50	0.48	134	31.9	617	−7.4	−42
	Max	26.0	8.32	7800	214	1440	117	247	424	0.39	3070	184	399	1250	131	6296	−0.8	−11
RHSs	Median	18.1	7.82	230	n.m.	10.4	6.06	2.19	45.9	0.03	11.0	1.00	12.0	144	n.m.	254	−7.0	−38
	Min	15.7	7.49	198	n.m.	5.52	2.74	1.22	41.5	0.02	9.22	0.50	0.96	85.4	n.m.	208	−7.4	−42
	Max	19.2	8.37	305	n.m.	14.3	17.2	6.68	49.3	0.06	16.3	44.0	57.6	177	n.m.	298	−6.9	−37

Sample		Li µg/l	B µg/l	Al µg/l	V µg/l	Cr µg/l	Mn µg/l	Fe µg/l	Co µg/l	Ni µg/l	Cu µg/l	Zn µg/l	As µg/l	Se µg/l	Rb µg/l	Sr µg/l	Mo µg/l	Cd µg/l	Sb µg/l	Cs µg/l	Ba µg/l	Pb µg/l	U µg/l
Paus.	Med	614	7685	1.20	8.45	5.00	813	57.9	1.82	1.42	21.8	11.5	2.65	0.50	264	8015	2.19	0.06	0.10	29.3	52.6	0.15	0.47
	Min	419	5110	0.50	4.36	0.50	123	28.6	1.40	0.50	0.50	7.26	0.54	0.11	158	5620	0.50	0.01	0.10	25.1	29.6	0.10	0.44
	Max	671	8210	54.1	71.3	9.50	1110	71.4	3.59	15.7	43.1	15.8	6.60	85.5	297	9150	3.88	0.10	0.10	33.5	72.1	0.19	0.50
Ag. Nik.	Med	558	2910	8.92	4.77	0.53	773	31.8	0.78	1.26	2.01	17.3	2.41	0.10	315	2900	0.50	0.02	0.10	50.1	5.49	0.28	0.25
	Min	463	2320	0.10	4.04	0.38	64.0	9.5	0.55	0.49	0.90	4.77	2.12	0.10	262	2210	0.20	0.02	0.03	42.8	2.38	0.05	0.17
	Max	585	3570	17.2	6.92	8.52	1200	87.1	1.72	1.78	3.57	61.4	3.25	0.50	374	3290	5.12	0.10	0.34	59.8	16.8	0.68	0.33
Loutra	Med	1480	10,300	21.1	6.41	2.29	2620	95.6	1.97	5.19	6.59	11.2	94.3	0.20	941	9580	1.30	0.10	0.09	179	60.0	1.20	1.13
	Min	663	3870	3.80	4.50	0.41	495	36.7	1.00	1.56	0.43	2.00	32.9	0.10	338	3690	0.46	0.03	0.01	71.7	25.8	0.38	0.84
	Max	1740	11,800	43.4	60.4	13.3	3280	758	2.14	25.6	66.1	17.0	284	50.1	1074	11,300	10.1	0.11	1.12	202	71.2	2.11	2.90
cold	Med	45.0	345	4.03	20.2	0.57	8.95	13.9	0.48	1.52	3.58	13.3	2.82	0.30	25.1	703	0.66	0.10	0.08	0.20	134	0.52	1.05
	Min	0.60	65.6	0.10	1.99	0.12	1.01	2.65	0.10	0.58	0.55	2.37	0.26	0.13	3.63	262	0.17	0.03	0.02	0.10	21.1	0.10	0.13
	Max	582	5820	18.9	69.9	3.88	2697	2086	48.0	37.1	41.6	211	13.7	0.54	175	3090	4.90	0.88	1.14	6.69	657	4.26	6.65

Cold GW = cold groundwaters; RHSs = Rainwater harvesting systems; n.m. = not measured.

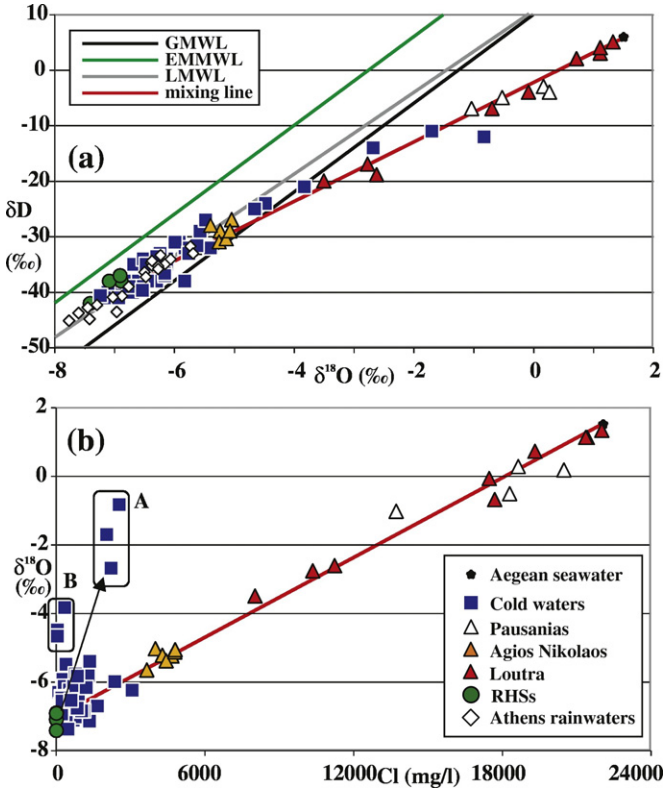

Fig. 2. Binary diagrams of δD vs. $\delta^{18}O$ (a) and $\delta^{18}O$ vs. Cl (b). EMMWL = Eastern Mediterranean Meteoric Water Line (Gat and Carmi, 1970), LMWL = Local Meteoric Water Line (Athens rainwater - Argiriou and Lykoudis, 2006 and IAEA, 2015), GMWL = Global Meteoric Water Line (Craig, 1961). Box A = waters affected by evaporation; Box B = waters belonging to very short hydrologic circuits (see text for further explainations).

peninsula. The outcropping terrain of the peninsula almost exclusively comprises volcanic rocks that contribute almost equally to the meteoric recharge of the aquifers. Therefore, either there is a sharp rainfall gradient that increases the contribution of the higher parts of the peninsula to the groundwater recharge, or the above-mentioned $\delta^{18}O$ lapse rate is not perfectly applicable to the Methana area. This clearly highlights the fact that lapse rates determined outside the study area should be applied with precaution and should be used mainly to highlight relative differences between the sampling points.

Samples with $\delta^{18}O$ values higher than −5.0‰ refer either to the above-described evaporated waters or to samples (e.g. B in Fig. 2b) collected in a restricted area on the eastern coast. The more-positive values of the latter samples are not due to either evaporative processes or mixing with seawater. The meteoric recharge of these two sampling sites is probably restricted by the low-altitude surroundings. A fault system made impermeable by previous hydrothermal activity (Rahders et al., 1997) isolates this area from higher elevation recharge.

4.2. Major-ion chemistry

All of the thermal waters at Methana have a Na-Cl composition, and on a Piper diagram (Fig. 3) their data appear close to the composition of Aegean seawater. The RHS samples display a Ca-HCO_3 composition, and are sometimes enriched in sulphate, which is a typical feature of rainwater in the Mediterranean area (D'Alessandro et al., 2013 and references therein). The cold groundwaters fall between the RHS, thermal water and Aegean seawater.

The way in which seawater influences both thermal and cold groundwaters is highlighted in the binary diagram of Na vs. Cl in Fig. 4a, where the data of nearly all samples appear on the line representing the Na/Cl ratio of the Aegean seawater. This influence can be due not only to direct seawater intrusion into both the thermal and cold aquifers, but also to contamination of the meteoric recharge by sea spray. The first process is probably responsible for most of the

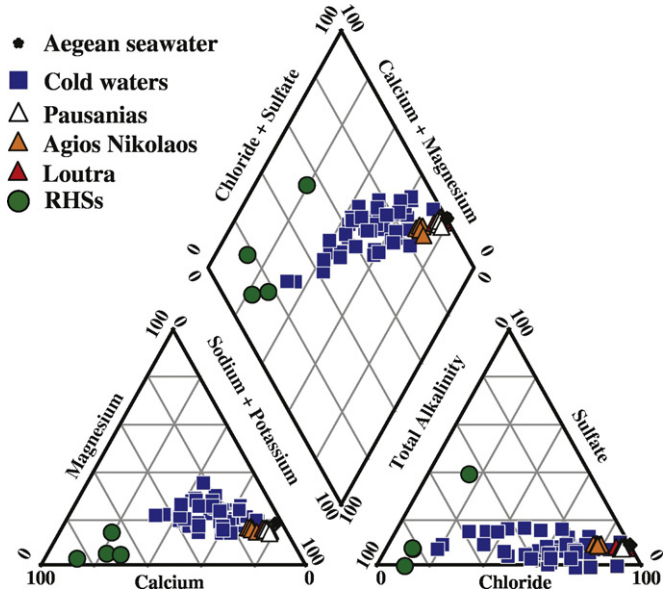

Fig. 3. Piper diagram showing the composition of the major ions in the sampled waters.

dissolved load in the waters displaying the highest salinities, while the second process becomes significant for the most-diluted ones. There is evidence of the contribution of sea spray at small islands (with which Methana can be compared) through meteoric recharge in the Aegean area (Dazy et al., 1997). The RHS samples display Na and Cl values that are within the range of composition of rainwaters collected close to the coast, but are lower than those measured at the Aegean islands (Dazy et al., 1997). This could be due to all of the sampled RHSs being located at sites that are not directly open to the sea. However, part of the recharge areas feeding the Methana aquifers are more exposed to sea-spray deposition, and the dry climatic conditions probably result in the infiltrating waters being further concentrated by evaporation processes prior to infiltration.

Chloride behaves as a conservative ion in the salinity range of the analysed waters, and so this ion is not affected by the precipitation of secondary minerals in the aquifers. For this reason its concentration was compared with those of all other analysed ions in binary diagrams in order to obtain insight into the processes affecting the mineralization of the waters (Fig. 4). The obtained ion/Cl^- ratios are almost always higher than the respective ion/Cl^- ratio in seawater, which indicates that the total ionic content of the water does not derive exclusively from mixing between the seawater and meteoric water end members. Water–rock interaction processes within the aquifer—which are further enhanced by the increased aggressiveness of the water due to the dissolution of endogenous CO_2 (D'Alessandro et al., 2008)—are responsible for the enrichment of nearly all major ions. The influence of CO_2 dissolution in the aquifer is also confirmed by the high alkalinity (Fig. 4d) and CO_2 partial pressure (D'Alessandro et al., 2008) values measured especially in the thermal waters. The aggressiveness of the thermal waters is possibly further enhanced by the addition of H_2S of hydrothermal origin and by the release of protons by its oxidation reaction in the shallowest part of the aquifer. Although the presence of H_2S is made evident by the smell of rotten eggs at the springs of Loutra, this process cannot be confirmed from the present data. The dissolved SO_4^{2-} deriving from H_2S oxidation is chemically not distinguishable from that deriving from seawater mixing or from the dissolution of hydrothermal-derived sulphate minerals. As demonstrated below the latter process contributes to a significant part of the dissolved SO_4 and $\delta^{34}S$ values (Dotsika et al., 2010) confirm that SO_4, though of prevailingly seawater origin, shows a contribution from a hydrothermal source.

A few exceptions to the enrichment of the ion/Cl^- ratio of seawater can be found for the Mg^{2+} and SO_4^{2-} contents of some of the sampled

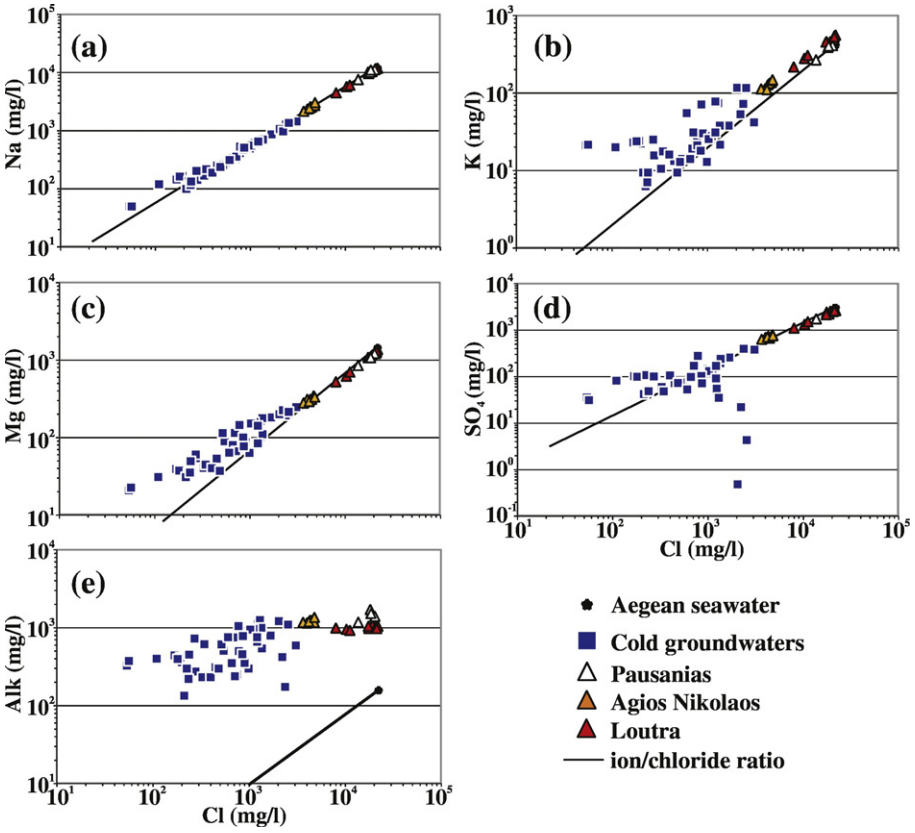

Fig. 4. Binary diagrams of Cl vs. (a) Na, (b) K, (c) Mg, (d) SO_4 and (e) alkalinity.

waters. In the case of Mg^{2+} (Fig. 4c), only the most-saline thermal waters display a small depletion, which can be attributed either to the incorporation of Mg^{2+} in secondary minerals or to dolomitization processes within the thermal aquifer. The depletion (or even occasional disappearance) of SO_4^{2-} evident in Fig. 4e affects only a few cold-groundwater samples. These samples were collected in the same wells in which the isotopic composition highlighted important evaporative processes. Our hypothesis is that in these shallow wells the decay of accumulated organic debris probably causes strongly negative redox potentials that lead to the reduction of SO_4^{2-} to H_2S. The latter escapes in gaseous form during evaporation processes or precipitates as sulphide minerals, leaving the water depleted in SO_4^{2-}.

Calcium is one of the major cations that is most enriched with respect to seawater, as indicated by a high ion/Cl^- ratio (Fig. 5a). Apart from dissolution of primary minerals in volcanic rocks, the high Ca^{2+} content could derive from carbonate rock dissolution. Only two of the sampled wells (samples 43 and 44 in Table S1) were excavated where Mesozoic carbonate rocks crop out, and the thermal springs of Loutra (samples 13 to 21 in Table S1) emerge at the contact between volcanics and limestones, but the geophysical investigation of Volti (1999) highlighted the presence of carbonate rocks under the volcanic products of the peninsula. The carbonate rocks extend under the entire peninsula at depths of less than about 1 km, and at least the aquifers feeding the thermal springs are partially composed of these rocks.

In the Ca-vs.-alkalinity binary diagram in Fig. 5b, most of the data for cold groundwaters appear along a line corresponding to the stoichiometric ratio of $CaCO_3$ dissolution. This could be due to dissolution of either limestones or calcite veins within the volcanic rocks. Important calcite mineralizations have been found in many hydrothermally altered volcanic rocks at the peninsula (Rahders et al., 1997). The most bicarbonate-rich cold groundwaters are depleted in Ca with respect to the ratio due to $CaCO_3$ dissolution. In these waters, which are either saturated or oversaturated with respect to calcite, the further addition of endogenous CO_2 and its titration to bicarbonate during water–rock interaction processes probably leads to the loss of Ca due to calcite precipitation.

The data for the waters collected at the Agios Nikolaos spring (samples 5 to 12 in Table S1), which are the thermal waters that are the least contaminated by seawater, fall on the $CaCO_3$ dissolution line (Fig. 5b). In contrast, the remaining data for thermal-water samples appear above this line, representing evidence for an additional source of Ca. In the Ca-vs.-SO_4 binary diagram in Fig. 5c, the data for these samples appear on a line corresponding to the stoichiometric ratio of $CaSO_4$ dissolution. Evaporitic rocks have never been described in the area (Dietrich and Gaitanakis, 1995; Volti, 1999), but the dissolution of hydrothermal anhydrite could explain the composition of these waters. Anhydrite is a common mineral in seawater-dominated hydrothermal systems (Bischoff and Seyfried, 1978), and its presence—together with other sulphate minerals—has been documented in the hydrothermal alteration products found at Methana (Rahders et al., 1997).

Nitrate concentrations in the Methana groundwaters are below the European Union (EU) drinking-water limit (50 mg/l) in all except seven of the samples, of which five were obtained from the same sampling site. The anomalous values were all found in the main village at Methana, implying that they probably originate from septic tanks rather than from the application of fertilizers.

4.3. Trace elements

The analysed trace elements show a wide range of concentrations (Fig. 6), with median values ranging from <0.1 μg/l (Cd and Sb) to >100 μg/l (B and Sr). The concentrations of most of the analysed trace elements (F, Li, B, Al, Cr, Mn, Fe, Co, As, Rb, Sr and Cs) are significantly higher in the thermal waters than in the cold groundwaters. The lower pH and the higher temperature and concentration of complexing agents (e.g., HCO_3^-, SO_4^{2-} and Cl^-) of the thermal waters favour the solubility of these elements. In contrast, the concentrations of only two elements (V and Ba) are significantly lower in the thermal waters than in the cold groundwaters. The solubility of V is favoured by slightly alkaline and oxidizing conditions (Wright and Belitz, 2010), which at Methana prevail in the cold groundwaters. The solubility of Ba in the thermal waters is restricted by barite saturation.

Ions of Fe and Mn are among the most enriched elements with respect to the ion/Cl^- ratio of seawater. They derive from the incongruent dissolution of femic minerals in the volcanic rocks at Methana. The negative redox conditions of most of the thermal waters at Methana further favours the solubility of these elements. Such strong enrichment is common in the geothermal systems along the south Aegean arc. For example, the thermal springs at Santorini and Milos islands that discharge directly in the sea are renowned for their high content of these elements (Boström et al., 1990; Cronan and Varnavas, 1999). The mixing with open seawater in these springs results in the abundant precipitation of Fe- and Mn-enriched sediments. Such sediments have also been found close to the Methana coast, providing evidence for past and/or present

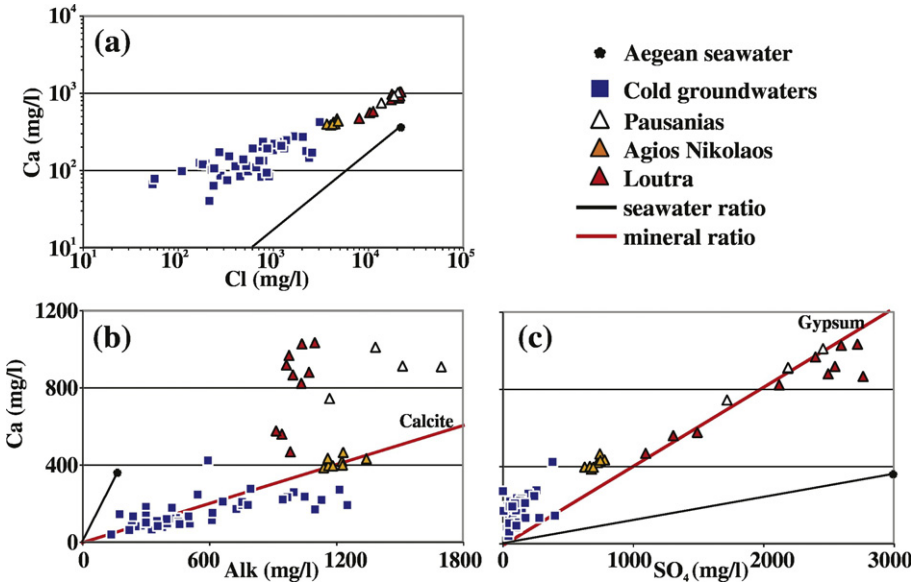

Fig. 5. Binary diagrams of Ca vs. (a) Cl^-, (b) alkalinity and (c) sulphate.

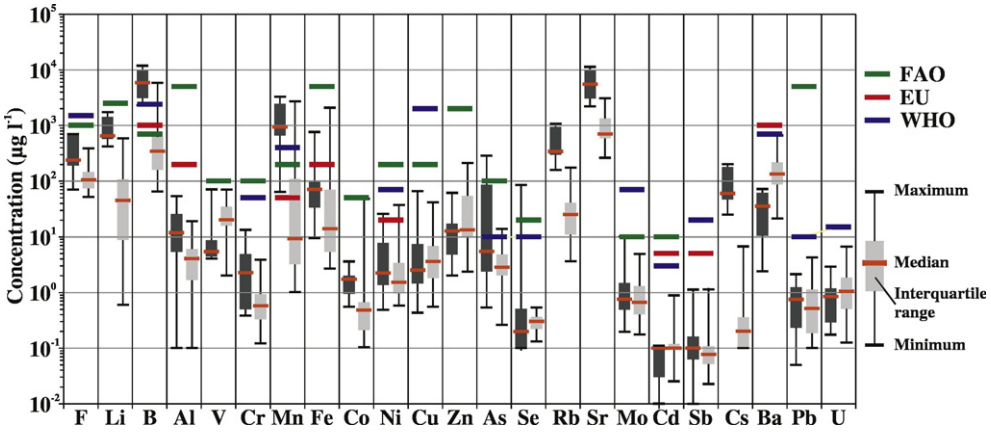

Fig. 6. Box-and-whiskers plot of the concentrations of minor and trace elements in the analysed groundwaters. Dark-grey and pale-grey boxes refer to thermal and cold groundwaters, respectively. Red and blue bars refer to the drinking-water limits set by the European Union (EU, 1998) and the World Health Organization (WHO, 2008) respectively. The green bar refers to the agricultural-water limits set by the Food and Agriculture Organization (Ayers and Westcot, 1985).

underwater hydrothermal discharge (Hübner et al., 2004), which is also evident from the bioaccumulation of these elements in algae growing in these areas (Baggini et al., 2014).

While the concentrations of some elements in the thermal waters at Methana exceed the limits set by the EU and the World Health Organization (WHO) for drinking water or by the Food and Agriculture Organization (FAO) for irrigation water (Fig. 6), they are not considered in the present discussion on water quality because these thermal waters are not used for either drinking or agriculture. Only a few of the cold groundwater samples exceed the above-mentioned limits (Fig. 6). The elements exceeding the limits are B, Mn, Fe, Ni and As, which points to a prevailing or even exclusive natural (hydrothermal) origin. Manganese exceeds the EU limit for drinking water (50 μg/l) in 15 out of 45 cases, reaching concentrations up to 2700 μg/l. However, this limit is based on the organoleptic quality rather than for protecting human health. Only four samples exceed the less-stringent limits of WHO (400 μg/l) and FAO (500 μg/l) related to human and plant health, respectively. Nine samples—of which three were obtained from the same sampling site—exceed the EU (1000 μg/l) and FAO (932 μg/l) limits for B, and are therefore unsuitable for drinking or irrigation.

It has to be highlighted that only 10 of the cold waters have salinities below the maximum recommended value (1.2 g/l – WHO, 2008) for drinking water. Nevertheless, some of the sampled waters, with salinities up to 1.5 g/l, are used as drinking waters by the owners of the wells. Among these waters only Mn exceeds in 3 cases the EU limit for drinking water (50 μg/l).

4.4. Salinity issues

The RHS samples show low salinities with EC values between 198 and 305 μS/cm, while the cold groundwaters show higher values that cover a wider range (734–7800 μS/cm; Table 1). Half of the samples show EC values higher than 2250 μS/cm, which is considered an upper limit for use in irrigation. High salinity is also related to high Na concentrations, which can be both toxic to plants and reduce the permeability of soil (Hanson et al., 2006). Issues related to both high salinities and Na contents in irrigation waters can be quantified using the salinity and sodicity hazard indexes as defined by Richards (1954). The salinity hazard index uses the EC value while the sodicity hazard index is based on the Na absorption ratio (SAR) defined by the following equation:

$$SAR = \frac{Na^{+}}{\sqrt{\left(Ca^{2+} + Mg^{2+}\right)/2}}$$

where the ion concentrations are expressed in milliequivalents per litre.

Both of these indexes are shown in Fig. 7, which includes grids indicating where problems occur with plant toxicity (Fig. 7a) and soil permeability (Fig. 7b). The only samples that fall in the low salinity and sodicity hazards classes are those from the RHSs. In contrast, the cold groundwaters span salinity hazard classes from medium to very high and sodicity hazard classes from low to very high (Fig. 7a), indicating the potential for toxicity to plants. In contrast, even the cold groundwaters with the highest SAR values do not represent a problem for soil permeability (Fig. 7b). This means that there is a low risk of salt accumulation in the shallow soil layers. Together with the intrinsic higher permeability of young volcanic soils, this probably greatly reduces toxicity problems in irrigated crops. Even waters with the worst salinity and sodicity indexes (sample 41 in Table S1) and very high B contents (samples 27 and 66 in Table S1) are used to irrigate vegetable gardens at Methana without evidence of plant distress, which is probably also related to salinity-resistant varieties being cultivated.

4.5. Hydrological model

No deep well exists on the peninsula and no exploration drilling has ever been made in this area. Hypothesis on the relative geometry of the outcropping rocks in the subsoil have been made only on the basis of geological and structural studies (Dietrich and Gaitanakis, 1995) and on limited geophysical measurements. Self-potential measurements and a geoelectric profile of 10 DC resistivity soundings have been made around the main thermal springs (Thanasoulas and Ksanthopoulos, 1991) and the suggested low-resistivity values (1–5 Ωm) for the top few hundred metres were explained mainly in terms of sea water intrusions. Thirteen magnetotelluric measurements along the entire peninsula gave insight up to depths of >5 km (Volti, 1999). All these informations have been summarised in the simplified geo-hydrological cross-section of Fig. 8. In the central part of the peninsula Volti (1999) found a high-resistivity area (>1500 Ωm) at shallow levels (<1 km). This suggests that groundwater circulation within the massive volcanics is limited in depth and that the cold aquifers are limited to the shallower scoriaceous parts of the volcanic domes, the drainage network in between the domes and to the coastal debris flow and alluvial fans (James et al., 1997). Continuity in space of such shallow cold aquifers is testified by isotopic composition indicating relatively high recharge altitudes. The presence of impermeable Flysch deposits of unknown thickness below the volcanics could also contribute to the high resistivity and represent the caprock of the hydrothermal

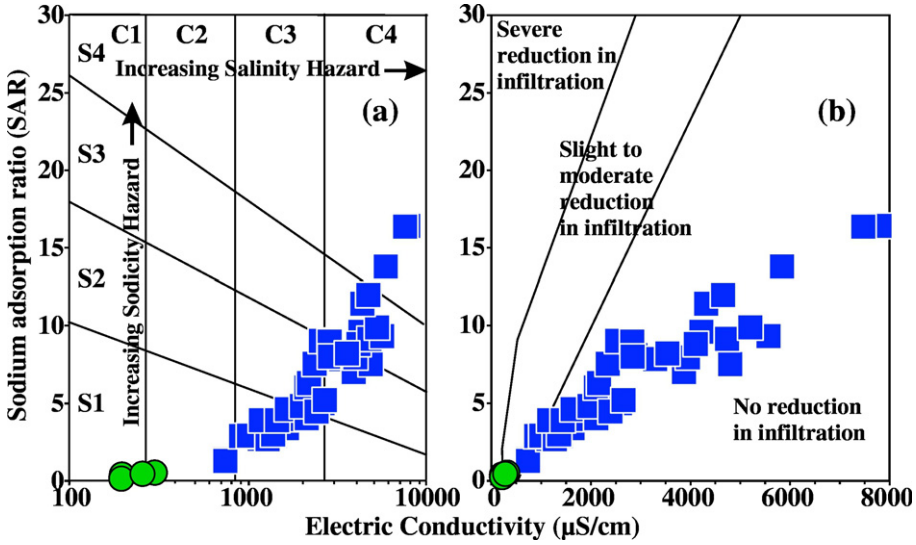

Fig. 7. Na absorption ratio (SAR) vs. electric conductivity, with grids indicating where problems occur with plant toxicity (a) and soil permeability (b).

reservoir. A conductive area (<30 Ωm) extending down to 5 km and with a minimum in resistivity of 7 Ωm at 2–3 km was found below. Volti (1999) interpreted such low-resistivity area as due to limestones fractured by volcanic intrusions and affected by intense circulation of fluids. Both limestones of Triassic and of Cretaceous age crop out on the peninsula and on the nearby areas. These could represent the aquifer rocks of the reservoir which is probably recharged by sea-water. The surface manifestations of this hydrothermal system are the three thermal springs of the peninsula where the thermal fluids come up through main tectonic features. As previously pointed out by D'Alessandro et al. (2008), sea-water contamination in the shallow part of the hydrothermal circuit makes the chemical composition of the thermal springs unsuitable for geothermometric estimations. Nevertheless the same authors obtained a reliable estimation of 200–220 °C from the composition of the gases released by the system confirming the presence of an active hydrothermal system.

5. Conclusions

The main process affecting the salinity of the Methana groundwaters is mixing between meteoric and seawater components. This process could be considered to originate naturally from the Methana peninsula being analogous to a small island and therefore affected by both direct seawater intrusion and sea-spray deposition. Thermal waters display the highest proportion of seawater (up to nearly 100%), with the intrusion of seawater into the thermal aquifer probably being a convective phenomenon, while salinization of the cold aquifer due to overextraction is a minor problem.

The compositions of groundwaters are modified when they circulate underground by water–rock interaction processes, which are enhanced by abundant endogenous CO_2 dissolution. Nearly all of the samples in the present study display ion/Cl^- ratios higher than those obtained from simple seawater addition. This indicates that the chemical

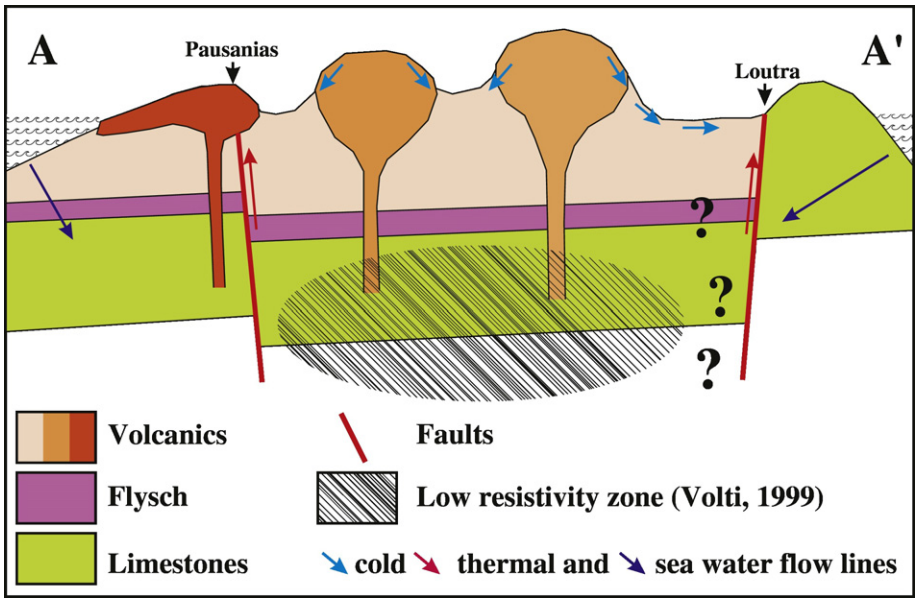

Fig. 8. Simplified geo-hydrologic profile of the peninsula of Methana. Due to the absence of deep exploration drillings, the reconstruction of the lithological sequence below the central part of the area is partially speculative although supported by the results of the magnetotelluric soundings made by Volti (1999).

evolution of the waters is modified by the dissolution of primary minerals of aquifer rocks. Dissolution of secondary hydrothermal minerals (calcite and anhydrite) sometimes also contributes to the chemistry of the thermal water, while precipitation of secondary minerals has only a minor impact on its chemistry.

Cold groundwaters are sometimes affected by substantial amounts of seawater that result in EC values and Na contents that would make them unsuitable for use in agriculture. However, even when the saltiest of the cold-groundwater samples found in the present study are used to irrigate crops, there are no evident signs of toxicity to plants. This is probably due to the cultivation of salinity-resistant crops and the presence of factors that do not support salt accumulation in soils (e.g. high permeability and a sufficiently deep water table).

The main parameter that limits the suitability of the cold waters of Methana is the salinity and only 10 samples out of 45 were below the maximum value fixed by the WHO (1.2 g/l). The main contaminants are mostly related to the hydrothermal activity of the area: B, Mn, Fe, Ni and As. The only anthropogenic contaminant in the cold groundwater is nitrate, whose concentration exceeds drinking water limits only in three wells within the main inhabited area of Methana.

Supplementary data to this article can be found online at http://dx.doi.org/10.1016/j.gexplo.2017.01.003.

Acknowledgments

We thank Giorgos Michas and Giorgos Papadakis for their friendly help in the field. We also thank the managers and employees of the spas of Loutra Methana and Agios Nikolaos and all the well owners who kindly gave us permission to sample their wells and particularly Mr. Alechos Vlachos. The insightful comments of two anonymous referees were appreciated.

References

Aiuppa, A., Bellomo, S., Brusca, L., D'Alessandro, W., Federico, C., 2003. Natural and anthropogenic factors affecting groundwater quality of an active volcano (Mt. Etna, Italy). Appl. Geochem. 18:863–882. http://dx.doi.org/10.1016/S0883-2927(02)00182-8.

Aiuppa, A., D'Alessandro, W., Gurrieri, S., Madonia, P., Parello, F., 2007. Hydrologic and geochemical survey of the lake "Specchio di Venere" (Pantelleria island, Southern Italy). Environ. Geol. 53, 903–913.

Argiriou, A.A., Lykoudis, S., 2006. Isotopic composition of precipitation in Greece. J. Hydrol. 327:486–495. http://dx.doi.org/10.1016/j.jhydrol.2005.11.053.

Ayers, R.S., Westcot, D.W., 1985. Water quality for agriculture. FAO Irrigation and Drainage Paper 29 (Rev. 1). Food and Agriculture Organization of the United Nations, Rome, p. 174.

Baggini, C., Salomidi, M., Voutsinas, E., Bray, L., Krasakopoulou, E., Hall-Spencer, J.M., 2014. Seasonality Affects Macroalgal Community Response to Increases in pCO_2. PLoS One 9, e106520. http://dx.doi.org/10.1371/journal.pone.0106520.

Bischoff, J.L., Seyfried, W.E., 1978. Hydrothermal chemistry of seawater. Am. J. Sci. 278, 838–860.

Boström, K., Perissoratis, C., Galanopoulos, V., Papavassiliou, C., Boström, B., Ingri, J., Kalogeropoulos, S., 1990. Geochemistry and structural control of hydrothermal sediments and new hot springs in the caldera of Santorini, Greece. In: Hardy, D.A., Boström, K. (Eds.), Proc. of the 3rd International Conference Thera and the Aegean World, Santorini, Greece, 1989, pp. 325–336.

Celico, P., Stanzione, D., Esposito, L., Formica, F., Piscopo, V., De Rosa, B., 1999. La complessità idrogeologica di un'area vulcanica attiva: l'Isola di Ischia (Napoli-Campania). Boll. Soc. Geol. Ital. 118, 485–504.

Cordeiro, S., Coutinho, R., Cruz, J.V., 2012. Fluoride content in drinking water supply in Sao Miguel volcanic island (Azores, Portugal). Sci. Total Environ. 432:23–36. http://dx.doi.org/10.1016/j.scitotenv.2012.05.070.

Craig, H., 1961. Isotopic variations in meteoric waters. Science 133, 1702–1708.

Cronan, D.S., Varnavas, S.P., 1999. Metalliferous sediments off Milos, Hellenic volcanic arc. Explor. Min. Geol. 8, 289–297.

Custodio, E., 2010. Coastal aquifers of Europe: an overview. Hydrogeol. J. 18:269–280. http://dx.doi.org/10.1007/s10040-009-0496-1.

D'Alessandro, W., Kyriakopoulos, K., 2013. Preliminary gas hazard evaluation in Greece. Nat. Hazards 69:1987–2004. http://dx.doi.org/10.1007/s11069-013-0789-5.

D'Alessandro, W., Federico, C., Longo, M., Parello, F., 2004. Oxygen isotope composition of natural waters in the Mt. Etna area. J. Hydrol. 296:282–299. http://dx.doi.org/10.1016/j.jhydrol.2004.04.002.

D'Alessandro, W., Brusca, L., Kyriakopoulos, K., Michas, G., Papadakis, G., 2008. Methana, the westernmost active volcanic system of the south Aegean arc (Greece): insight from fluids geochemistry. J. Volcanol. Geotherm. Res. 178:818–828. http://dx.doi.org/10.1016/j.jvolgeores.2008.09.014.

D'Alessandro, W., Bellomo, S., Bonfanti, P., Brusca, L., Longo, M., 2011. Salinity variations in the water resources fed by the Etnean volcanic aquifers (Sicily, Italy): natural vs. anthropogenic causes. Environ. Monit. Assess. 173:431–446. http://dx.doi.org/10.1007/s10661-010-1397-4.

D'Alessandro, W., Katsanou, K., Lambrakis, N., Bellomo, S., Brusca, L., Liotta, M., 2013. Chemical and isotopic characterisation of bulk deposition in the Louros Basin (Epirus, Greece). Atmos. Res. 132–133:399–410. http://dx.doi.org/10.1016/j.atmosres.2013.07.007.

Dazy, J., Drogue, C., Charmanidis, P., Darlet, C., 1997. The influence of marine inflows on the chemical composition of groundwater in small islands: the example of the Cyclades (Greece). Environ. Geol. 31, 133–141.

Dietrich, V., Gaitanakis, P., 1995. Geological map of Methana peninsula (Greece). ETH Zürich, Switzerland.

Dotsika, E., Poutoukis, D., Raco, B., 2010. Fluid geochemistry of the Methana Peninsula and Loutraki geothermal area, Greece. J. Geochem. Explor. 104:97–104. http://dx.doi.org/10.1016/j.gexplo.2010.01.001.

Duriez, A., Marlin, C., Dotsika, E., Massault, M., Noret, A., Morel, J.L., 2008. Geochemical evidence of seawater intrusion into a coastal geothermal field of central Greece: example of the Thermopylae system. Environ. Geol. 54, 551–564.

EU, 1998. Council Directive 98/83/EC/9-11-1998/ on the quality of water intended for human consumption. Official Journal of the European Communities, No. L330/32-54/5-12-98.

Forbes, H., 1997. Turkish and modern Methana. In: Mee, C., Forbes, H. (Eds.), A Rough and Rocky Place. Liverpool University Press.

Francalanci, L., Vougioukalakis, G.E., Perini, G., Manetti, P., 2005. A west-east traverse along the magmatism of the south Aegean volcanic arc in the light of volcanological, chemical and isotope data. In: Fytikas, M., Vougioukalakis, G.E. (Eds.), The South Aegean Active Volcanic Arc 7. Developments in Volcanology, pp. 65–111.

Freire, P., Andrade, C., Coutinho, R., Cruz, J.V., 2014. Spring geochemistry in an active volcanic environment (São Miguel, Azores): Source and fluxes of inorganic solutes. Sci. Total Environ. 466–467:475–489. http://dx.doi.org/10.1016/j.scitotenv.2013.06.073.

Fytikas, M., Innocenti, F., Kolios, N., Manetti, P., Mazzuoli, R., 1986. The Plio-Quaternary volcanism of the Saronikos area (western part of the active Aegean volcanic arc). Ann. Géol. Pays Hellén. 33, 23–45.

Gat, J.R., Carmi, I., 1970. Evolution of the isotopic composition of atmospheric waters in the Mediterranean Sea area. J. Geophys. Res. 75, 3039–3048.

Grassi, S., Squarci, P., D'Amore, F., Mussi, M., 1995. Circulation of thermal waters of Pantelleria Island (Sicily Channel, Italy). Proc. World Geothermal Congress, Florence 18–31 May 1995. vol. 2, pp. 703–706.

Hanson, B.R., Grattan, S.R., Fulton, A., 2006. Agricultural salinity and drainage. Division of Agriculture and Natural Resources Publication 3375, University of California Irrigation Program. University of California, Davis, U.S.A., p. 164.

Hübner, A., Rahders, E., Rahner, S., Halbach, P., Varnavas, S.P., 2004. Geochemistry of hydrothermally influenced sediments off Methana (western Hellenic volcanic arc). Chem. Erde 64:75–94. http://dx.doi.org/10.1016/j.chemer.2003.10.001.

IAEA, 2015. Global Network of Isotopes in Precipitation GNIP-WISER Database. Available at: http://www-naweb.iaea.org/napc/ih/IHS_resources_isohis.html (accessed 29 Apr. 2016).

James, P., Atherton, M., Harvey, A., Firmin, A., Morrow, A., 1997. The physical environment of Methana: formation, exploitation and change. In: Mee, C., Forbes, H. (Eds.), A Rough and Rocky Place. Liverpool University Press, pp. 5–32.

Jung, H.-W., Yun, S.-T., Kim, K.-H., Oh, S.-S., Kang, K.-G., 2014. Role of an impermeable layer in controlling groundwater chemistry in a basaltic aquifer beneath an agricultural field, Jeju Island, South Korea. Appl. Geochem. 45:82–93. http://dx.doi.org/10.1016/j.apgeochem.2014.03.008.

Koh, D.-C., Ko, K.-S., Kim, Y., Lee, S.-G., Chang, H.-W., 2007. Effect of agricultural land use on the chemistry of groundwater from basaltic aquifers, Jeju Island, South Korea. Hydrogeol. J. 15, 727–743.

Kontis, E.E., Gaganis, P., 2012. Hydrochemical characteristics and groundwater quality in the island of Lesvos, Greece. Global NEST J. 14, 422–430.

Kuiper, N., Rowell, C., Shomar, B., 2015. High levels of molybdenum in Qatar's groundwater and potential impacts. J. Geochem. Explor. 150:16–24. http://dx.doi.org/10.1016/j.gexplo.2014.12.009.

Lambrakis, N., Kallergis, G., 2005. Contribution to the study of Greek thermal springs: hydrogeological and hydrochemical characteristics and origin of the thermal waters. Hydrogeol. J. 13:506–521. http://dx.doi.org/10.1007/s10040-004-0349-x.

Makris, J., Papoulia, J., Drakatos, G., 2004. Tectonic deformation and microseismicity of the Saronic Gulf, Greece. Bull. Seismol. Soc. Am. 94, 920–929.

Matiatos, I., Alexopoulos, A., 2011. Application of stable isotopes and hydrochemical analysis in groundwater aquifers of Argolis Peninsula (Greece). Isot. Environ. Health Stud. 47, 512–529.

Mee, C., Forbes, H. (Eds.), 1997. A Rough and Rocky Place: the Landscape and Settlement History of the Methana Peninsula. Liverpool University Press, Greece.

Milnes, E., Renard, P., 2004. The problem of salt recycling and seawater intrusion in coastal irrigated plains: an example from the Kiti aquifer (southern Cyprus). J. Hydrol. 288: 327–343. http://dx.doi.org/10.1016/j.jhydrol.2003.10.010.

Minissale, A., Duchi, V., Kolios, N., Nocenti, M., Verrucchi, C., 1997. Chemical patterns of thermal aquifers in the volcanic islands of the Aegean arc, Greece. Geothermics 26, 501–518.

Pantelouris, E.M., 1980. Greece: an introduction. Moffat.

Parkhurst, D.L., Appelo, C.A.J., 2010. User's Guide to PHREEQC (Version 2)-A Computer program for Speciation, Batch-Reaction, One-Dimensional Transport and Inverse Geochemical Calculations. Available at: ftp://brrftp.cr.usgs.gov/pub/charlton/phreeqc/Phreeqc_2_1999_manual.pdf (accessed 29 Apr. 2016).

Pe-Piper, G., Piper, D.J.W., 2002. The Igneous Rocks of Greece. Bornträger, Berlin.

Pertessis, M.L., 1925. Les eaux minerales de Methana. Publ. Bureau Geol, Athens.

Petalas, C., Lambrakis, N., 2006. Simulation of intense salinization phenomena in coastal aquifers: the case of the coastal aquifers of Thrace. J. Hydrol. 342, 51–64.
Petalas, C., Lambrakis, N., Zaggana, E., 2006. Hydrochemistry of waters of volcanic rocks: the case of the volcanosedimentary rocks of Thrace, Greece. Water Air Soil Pollut. 169, 375–394.
Rahders, E., Halbach, P., Halbach, M., Rahner, S., Varnavas, S.P., 1997. Hydrothermal alteration and precipitation processes on Methana peninsula, Greece. In: Papunen, H. (Ed.), Mineral Deposits: Research and Exploration, Where Do They Meet?Balkema, pp. 965–966.
Richards, L.A., 1954. Diagnosis and improvement of saline and alkaline soils. U.S. Salinity Laboratory Staff, Agricultural Handbook No 60. U.S. Department of Agriculture, p. 160.
Salama, R.B., Otto, C.J., Fitzpatrick, R.W., 1999. Contributions of groundwater conditions to soil and water salinization. Hydrogeol. J. 7, 46–64.
Stothers, R.B., Rampino, M.R., 1983. Volcanic eruptions in the Mediterranean before A.D. 630 from written and archeological sources. J. Geophys. Res. 88, 6357–6371.
Thanasoulas, K., Ksanthopoulos, N., 1991. A geophysical survey in Methana Peninsula - implication on the thermal springs (in Greek). Final report, Institute of Geological and Mineral Exploration (I.G.M.E.), Greece.
Volti, T.K., 1999. Magnetotelluric measurements on the Methana peninsula (Greece): modelling and interpretation. Tectonophy 301, 111–132.
von Leyden, R., 1940. Der Vulkanismus des Golfes von Ägina und seine Beziehungen zur Tektonik. Vulkaninstitut Immanuel Friedländer No 1, Zürich.
WHO, 2008. Drinking-water quality. Third ed. Vol. 1: Recommendations. World Health Organization, Geneva, p. 688.
Wright, M.T., Belitz, K., 2010. Factors controlling the regional distribution of Vanadium in groundwater. Ground Water 48, 515–525.
Zhang, W., Chen, X., Tan, H., Zhang, Y., Cao, J., 2015. Geochemical and isotopic data for restricting seawater intrusion and groundwater circulation in a series of typical volcanic islands in the South China Sea. Mar. Pollut. Bull. 93:153–162. http://dx.doi.org/10.1016/j.marpolbul.2015.01.024.